A STUDY OF INTER-SPACECRAFT COULOMB FORCES AND IMPLICATIONS FOR FORMATION FLYING

Lyon B. King, Gordon G. Parker, Satwik Deshmukh, and Jer-Hong Chong
Michigan Technological University, Houghton, MI 49931

ABSTRACT

In the course of exploiting spacecraft formations for use in separated interferometry (or other missions), it is possible that the separation distance between vehicles will be on the order of ten meters. This paper investigates the effects of spacecraft charging on the dynamics of very closely spaced formations. For certain high Earth orbits, the ambient plasma conditions will conspire to produce significant spacecraft charging in an environment with a plasma Debye length of more than 100 m. For such conditions, this paper shows the potential to develop disruptive inter-spacecraft Coulomb forces and torques with magnitude comparable to candidate formation-keeping thrusters over distances of tens of meters. Owing to the unexpectedly large interaction forces, the paper also explores the concept of purposely charging spacecraft to affect formation-keeping Coulomb forces. Analytic methods are developed that show the existence of static equilibrium formations in Earth orbit using only inter-vehicle Coulomb forces for one- two- and three-dimensional formations. Such Coulomb formations would be free of the risk of plume contamination due to thrusters firing in close proximity. Figures of merit for the proposed Coulomb control system are calculated analogous to traditional propulsion systems and it is shown that required forces can be created with milliwatts of power, can be controlled on a millisecond time scale, and imply specific impulse that can be as high as 10^{13} seconds.

1. Introduction

Swarms of microsatellites are envisioned as an alternative to traditional large spacecraft. Such swarms, acting collectively as virtual satellites, will benefit from the use of cluster orbits where the satellites fly in a close formation.[1] The formation concept, first explored in the 1980's to allow multiple geostationary satellites to share a common orbital slot,[2,3] has recently entered the era of application with many missions slated for flight in the near future. The promised payoff of formation-flying has recently inspired a large amount of research in an attempt to overcome the rich technical problems. A variety of papers can be found in the proceedings of the 1999 AAS/AIAA Space Flight Mechanics Meeting,[4,5,6] the 1998 Joint Air Force/MIT Workshop on Satellite Formation Flying and Micro-Propulsion,[7] a recent textbook on micropropulsion,[8] and numerous other sources.[9,10,11,12,13,14,15]

Relative position control of multiple spacecraft is an enabling technology for missions seeking to exploit satellite formations. Of the many technologies that must be brought to maturity in order to realize routine formation flying, perhaps the most crucial is the spacecraft propulsion system. The most challenging propulsion system demands will be made in close formations where inter-vehicle spacing may be as small as five or ten meters. Apart from the obvious danger of collision, exhaust plume contamination of sensitive instruments is a legitimate concern for spacecraft in a formation. In close proximity, the propellant emitted by such devices as micro-PPT's (vaporized Teflon), FEEP (ionized cesium), or colloid thrusters (liquid glycerol droplets doped with NaI) may impinge upon neighboring vehicles with the potential to damage payloads. To worsen the problem, orbital mechanics for many clusters of interest mandate continuous thruster firings pointed directly towards other vehicles in the formation.

Work reported in this paper represents what the authors believe is a new mode of propulsive interaction between spacecraft in close formation.

The interaction arises from Coulomb forces between vehicles in a swarm of electrically charged spacecraft. Forces can be produced as a result of natural charging due to space plasma interaction. In the case of natural charging, the Coulomb forces represent perturbations on vehicles in the formation, which on-board thrusters must counteract. It will be shown in following sections that, in high orbits such as GEO, natural charging is capable of producing forces and torques with magnitudes comparable to those of microthrusters over separation length scales of tens of meters.

In addition to an analysis of parasitic Coulomb forces from space plasma interaction, this paper reports on an exploratory study to examine the feasibility of using Coulomb forces to maintain rigid satellite formations in high earth orbit. In the Coulomb control scenario, on-board power would be used to actively charge vehicles in a swarm to affect formation-keeping forces and possibly act as an emergency collision avoidance system. The use of Coulomb forces would provide nearly propellantless formation control with little or no risk of exhaust plume contamination of neighboring vehicles. Analytic and numeric calculations show that the dynamic equations permit rigid Coulomb formations in orbit and that these formations are controllable in three dimensions. It is also shown that the amount of on-board power required to affect charge control is negligible and that continuous thrust variation is possible over rapid time scales.

2. Coulomb Perturbations

2.1. GEO Plasma Environment

The Coulomb force between two point charges in the presence of a plasma is represented by the typical inverse square relationship modified by an exponential term to account for the Debye shielding

Eqn. 1
$$F_{1,2} = \frac{1}{4\pi\varepsilon_0}\frac{q_1 q_2}{d_{1,2}^2}\exp\left(\frac{-d_{1,2}}{l_d}\right),$$

Where q_1,q_2 are the charges, $d_{1,2}$ is the separation distance, and l_d is the plasma Debye length. The potential for interaction between charged spacecraft is then limited to regimes in which the separation between vehicles is less than the plasma Debye length. Since the Debye length in low-Earth orbit (LEO) is on the order of centimeters, Coulomb interaction will be present only in high-earth orbits. Analysis in this study will be limited to geostationary Earth orbit (GEO) to take advantage of the wealth of plasmaphysical data available for GEO conditions.

An excellent discussion of the space plasma environment can be found in the textbook by Hastings and Garret,[16] some of which is repeated here for convenience. A spacecraft at GEO is at the edge of plasmapause. This collisionless plasma does not follow a single Maxwellian distribution. Instead, plasma parameters must be measured experimentally. The particle detectors on the ATS[17,18,19] and SCATHA[20] spacecraft have measured plasma variations between 5-10 eV and 50-80 eV approximately, for 50 complete days at 1 to 10 minute resolution from 1969 through 1980, bracketing one solar cycle.

Garrett and Deforest[17] fitted an analytical two-temperature model to data collected over 10 different days from ATS-5 spacecraft between 1969 and 1972. These data were selected in such a way to show a wide range of geomagnetic activity including plasma injection events (i.e. sudden appearance of dense, relatively high energy plasma at GEO occurring at local midnight). The model gives reasonable and consistent representation of the variations following a substorm injection event at GEO. The parameters for this model during average GEO conditions are shown in Table 1 with "Worst-case" GEO conditions given in Table 2. Calculations based on these parameters show that the Debye length at GEO ranges from about 140 m to greater than 1400 m.

Parameter	Electrons	Ions
n_1 (m^{-3})	0.78×10^6	0.19×10^6
kT_1/e (eV)	550	800
n_2 (m^{-3})	0.31×10^6	0.39×10^6
kT_2/e (eV)	8.68×10^3	15.8×10^3

Table 1. Average GEO environment.[17]

Parameter	Electrons	Ions
n_1 (m^{-3})	1×10^6	1.1×10^6
kT_1/e (eV)	600	400
n_2 (m^{-3})	1.4×10^6	1.7×10^6
kT_2/e (eV)	2.51×10^4	2.47×10^4

Table 2. Worst-case GEO environment.[17]

2.2. Modelling Spacecraft Charging

Spacecraft charging, especially differential charging, has been of prime concern to spacecraft designers because of its detrimental effects such as

electrostatic discharge in spacecraft and spacecraft subsystems. The NASA Space Environment Effects (SEE) Interactive Spacecraft Charging Handbook[21] is one of the tools available to model the plasma environment and spacecraft charging. The SEE tool allows specification of plasma parameters, spacecraft size, materials, and charging time, whereupon the program predicts potentials of elements on the spacecraft surface. The transient response of a spacecraft in plasma is calculated by modeling the spacecraft – ambient plasma system as an equivalent electric circuit. The equilibrium charge of a vehicle is obtained from the SEE model as the transient solution reaches steady state.

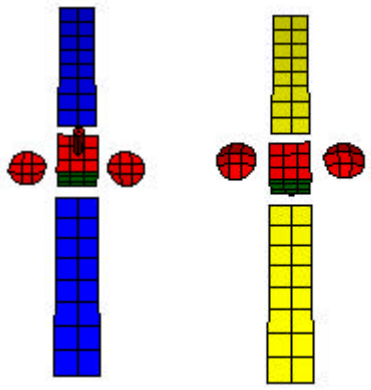

Component	Color	Size	Material
Chassis	Red Green	1mx1mx1m	Kapton OSR
Solar Arrrays	Blue Yellow	1mx4m	Solar Cells Black Kapton
Antennae	Red	1-m-dia.	Kapton
Omni Antenna	Red	0.2-m-dia. 1-m-long	Kapton

Figure 1. Spacecraft model used in SEE code seen from sun direction (left) and from opposite direction (right) with representative materials of each component.

The SEE code was used to predict spacecraft charging, with the intent of using the results of the SEE predictions to calculate Coulomb perturbations. The default spacecraft materials of the SEE code were used for these tests, which are shown in Figure 1. The SEE code has three pre-loaded GEO plasma environments, namely Worst-Case environment, ATS-6 environment and 4Sept97 environment. The specifications of these environments are given in Table 3. A representative solution from the SEE tool is shown in Figure 2. This figure shows the surface potential distribution (in units of volts) as a color-contour map.

Parameter	Worst-case	ATS-6	4-Sept.-97
n_e (m^{-3})	1.2×10^6	1.22×10^6	3.00×10^5
T_e (eV)	1.2×10^3	1.6×10^6	0.4×10^3
n_i (m^{-3})	2.36×10^5	2.36×10^5	0.30×10^5
T_i (eV)	2.95×10^3	2.95×10^3	0.40×10^3

Table 3. Parameters of the three pre-loaded GEO plasma environments in the SEE Interactive Spacecraft Charging Handbook.

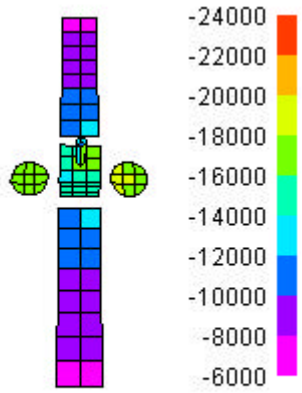

Figure 2. SEE prediction of spacecraft surface potentials for vehicle subject to worst-case GEO plasma environment in non-eclipse conditions. Units are volts.

2.3. Natural Forces and Torques

The output of the SEE model includes a value of potential for each finite element of the spacecraft surface. Using a vacuum Green's function

Eqn. 2
$$4\pi\varepsilon_0 V_i = \sum_j \frac{q_j}{\vec{r}_{ij}}$$

it is possible to calculate the equivalent point charge at the center of each finite element that is self consistent with the potential distribution. The interaction between two charged spacecraft can then be modeled as a superposition of the interactions of the equivalent point charges. For example, the collection of charges on spacecraft 'B' will produce an electric field at a point 'i' on spacecraft 'A' according to

Eqn. 3
$$\vec{E}_i = \frac{1}{4\pi\varepsilon_0} \sum_{j=1}^{nB} \frac{q_j \vec{r}_{ij} \exp\left(-\left|\vec{r}_{ij}\right| / l_d\right)}{\left|\vec{r}_{ij}\right|^3}$$

where n_B is the number of elements (charges) on spacecraft 'B'. If there is an electric charge q_i at 'i' it will experience a force $\vec{F}_i = q_i \vec{E}_i$. The net force on spacecraft 'A' resulting from the n_B charges on spacecraft 'B' is then simply

Eqn. 4
$$\vec{F}_{AB} = \sum_{i=1}^{nA} \vec{F}_i \,.$$

Using the same equivalent point charge method it is also straightforward to compute the moment on the charged spacecraft 'A' about its geometric center resulting from the distribution of charges on spacecraft 'B'.

The Coulomb interaction between closely spaced satellites was performed using the SEE code to predict the charging of representative spacecraft. Two identical vehicles, with material properties and physical dimensions as shown in Figure 1, were assumed to be in GEO separated along the direction of orbital velocity to mimic a leader-follower type of formation. The relative orientation of the vehicles is indicated in Figure 3.

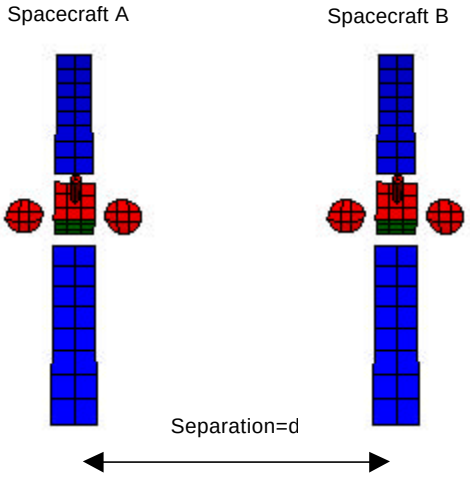

Figure 3. Relative orientation of two-spacecraft leader-follower formation for natural Coulomb interaction study. The vehicles are displaced only along the orbital velocity direction.

Three GEO plasma environments (see Table 3) were used to predict the spacecraft charging in both eclipse and non-eclipse conditions due to natural plasma interaction. The forces and torques were computed based on the SEE results for a range of spacecraft separations from 10 to 100 meters. The resulting inter-spacecraft forces and torques about geometric center are shown in Figure 4. The Coulomb interaction forces were found to be as large as 1 mN for spacecraft 10 m apart in the ATS-6 eclipse environment, with all environments except the 4-Sept.-97 case showing interaction forces greater than 10 μN at the closest spacing. The decay in force with separation is not purely $1/r^2$ due to the finite size effects of the vehicles. At the largest spacing considered (100 m) the inter-spacecraft forces vary from 10^{-10} N up to about 100 nN, depending upon the orbital conditions used in the SEE prediction. The electric-dipole-induced torques were found to be as large as 100 μN-m for the closest spacing in the ATS-6 Eclipse conditions, falling as low as 10^{-10} N-m for the 4-Sept.-97 case at 100-m spacing.

A surprising result of the Coulomb interaction study was that the magnitude of the inter-spacecraft forces is comparable with and may exceed that of candidate micropropulsion systems proposed for formation keeping. One method for eliminating the parasitic Coulomb forces and torques would be to actively control the spacecraft charge and ensure that vehicle potential remains very near the ambient plasma potential. This could be performed using a hollow-cathode plasma contactor as used on the International Space Station (ISS). Another interesting concept, however, is to use an ion or electron emitter to actively control the spacecraft charge and, thus, the Coulomb force to affect relative propulsion within a formation. The feasibility of forming Coulomb-stabilized formations will be the focus of Section 3.

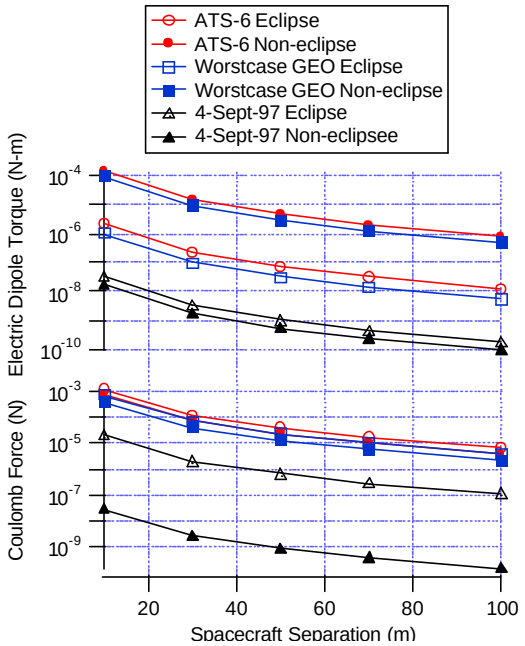

Figure 4. Predicted inter-spacecraft Coulomb force for two identical satellites in a GEO leader-follower formation as a function of the formation spacing.

3. Formation Dynamics

This section presents a summary of Coulomb formation dynamics that can be found in much more detail in the references.[22] Analytic methods are presented for determining static (rigid) formations of spacecraft flying in close proximity using inter-vehicle Coulomb forces to offset orbital perturbations. The vehicles are approximated as spheres and it is assumed that the plasma Debye length is much longer than a typical inter-vehicle separation. Such conditions are a reasonable approximation of formations in GEO with vehicle spacing on the order of tens of meters.

3.1. Dynamic Equations

As in many formation studies, Hill's equations are used here to describe the motion of spacecraft in a formation relative to a reference point that is assumed to maintain a circular Keplerian orbit. With an application slanted towards separated spacecraft interferometry, the central reference vehicle is referred to as a "combiner" where the surrounding vehicles are called "collectors". It is assumed that the combiner has its own station keeping system, but the collectors do not. Thus the only external forces on the collectors are the Coulomb interactions between them and the combiner.

Within the Hill's system, the motion of the *i*'th collector with respect to the central combiner-fixed coordinate system can be written for a formation of *n* vehicles interacting via Coulomb forces as

Eqn. 5

$$\ddot{x}_i - 2\Omega\dot{y}_i - 3\Omega^2 x_i = \frac{k_c}{m_i}\sum_{j=0}^{n}\frac{(x_i - x_j)}{\left|\vec{p}_i - \vec{p}_j\right|^3} q_i q_j$$

$$\ddot{y}_i + 2\Omega\dot{x}_i = \frac{k_c}{m_i}\sum_{j=0}^{n}\frac{(y_i - y_j)}{\left|\vec{p}_i - \vec{p}_j\right|^3} q_i q_j$$

$$\ddot{z}_i + \Omega^2 z_i = \frac{k_c}{m_i}\sum_{j=0}^{n}\frac{(z_i - z_j)}{\left|\vec{p}_i - \vec{p}_j\right|^3} q_i q_j$$

$$i = 1,\ldots,n \text{ and } i \neq j$$

where $\vec{p}_i$ denotes the position vector of the *i*'th vehicle, m_i is the spacecraft mass, Ω is the orbital angular velocity, q_i is the vehicle charge in Coulombs, and k_c=1/4pe_0 is Coulomb's constant. The coordinate notation is such that the y direction is along the orbital velocity vector, x is in the zenith-nadir direction, and z is normal to the orbit plane. The axis system is shown in Figure 5. The interesting difference between this set of equations and the typical Hill's system used in formation studies lies in their coupling: the dynamics of any vehicle in the formation is influenced simultaneously by all of the other vehicles in the group.

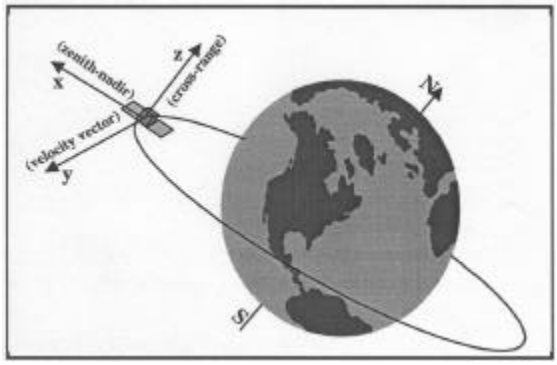

Figure 5. Illustration of combiner-fixed relative coordinate system used in the Hill's equation formulation (Figure reprinted from Ref. 23).

A static (rigid) formation geometry must satisfy the Hill's system of Eqn. 5 with zero relative velocity and acceleration for each vehicle ($\dot{x} = \ddot{x} = \dot{y} = \ddot{y} = \dot{z} = \ddot{z} = 0$). The nature of the Coulomb coupling of the system stipulates that control forces can only be applied along the lines "connecting" spacecraft coordinates. Thus, the goal is to find suitable formation geometries such that the vector sum of the Coulomb forces is sufficient to enable solution of the Hill's system with velocities and accelerations set to zero. The equilibrium system of equations is then found to be

$$-3\Omega^2 x_i = \frac{k_c}{m_i}\sum_{j=0}^{n}\frac{(x_i - x_j)}{\left|\vec{p}_i - \vec{p}_j\right|^3}q_i q_j$$

$$0 = \frac{k_c}{m_i}\sum_{j=0}^{n}\frac{(y_i - y_j)}{\left|\vec{p}_i - \vec{p}_j\right|^3}q_i q_j$$

Eqn. 6

$$\Omega^2 z_i = \frac{k_c}{m_i}\sum_{j=0}^{n}\frac{(z_i - z_j)}{\left|\vec{p}_i - \vec{p}_j\right|^3}q_i q_j$$

$$i = 1,\ldots,n \text{ and } i \neq j$$

3.2. ***Formation Geometries***

The method chosen for exploring the behavior of Eqn. 6 was to assume geometric formations and search for solution sets. Although numerous formations were studied in the reference work,[22] discussion here will be limited to three canonical cases. The first case considered was a simple linear three-vehicle formation with vehicles separated by L. With the combiner fixed to the origin, three sub-formations follow depending upon orientation with the axis system. The linear formations are shown in Figure 6.

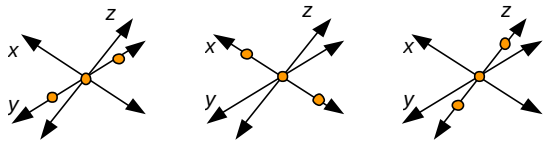

Figure 6. Linear three-spacecraft formations.

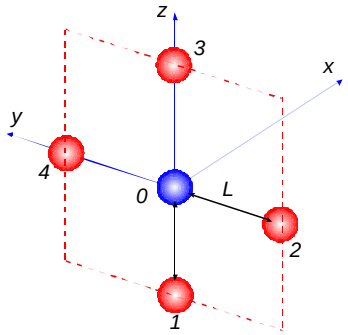

Figure 7. Illustration of the five-satellite formation.

The second formation studied was a simple two-dimensional formation that suggests an application for Earth observation through separated spacecraft interferometry. This configuration is shown in Figure 7, where the four collectors are distributed evenly about the Hill's y and z axes to create a five-spacecraft planar formation. The third formation represented a three-dimensional configuration, with six collectors distributed evenly about the principal axes with spacing L. The three-dimensional formation is shown in Figure 8.

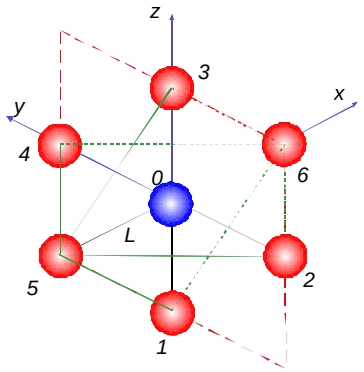

Figure 8. Illustration of seven-satellite formation.

3.3. ***Equilibrium Formation Solutions***

Although results will be presented for all of the formations outlined above, the analytic solution method will be presented only for the representative three-spacecraft x-axis aligned case, which we call the "Coulomb tether" due to its similarity with physical tether configurations. For three spacecraft aligned along the combiner coordinate frame's *x*-axis as shown in Figure 6, *n*=3 and the following relative displacement constraints hold

Eqn. 7

$$x_1 = L$$
$$x_2 = -L$$
$$y_1 = y_2 = z_1 = z_2 = 0$$

where *L* is the distance from the combiner to either collector. Forming all six of the equilibrium equations from Eqn. 6 and eliminating duplicate equations leaves only two conditions:

Eqn. 8

$$\frac{k_c q_1 q_2}{4L^2} + \frac{k_c q_1 q_0}{L^2} + 3m_1 L\Omega^2 = 0$$

Eqn. 9
$$\frac{k_c q_1 q_2}{4L^2} + \frac{k_c q_2 q_0}{L^2} + 3m_2 L\Omega^2 = 0$$

If we further assume that the collectors have equal mass, $m=m_1=m_2$ and introducing the normalized charges defined by

Eqn. 10
$$q_{in} \equiv \frac{q_i}{\sqrt{m_i L^3}}$$

allows Eqn. 8 and Eqn. 9 to be written without explicit mass and length dependencies

Eqn. 11
$$\frac{k_c q_{1n} q_{2n}}{4} + k_c q_{1n} q_{0n} + 3\Omega^2 = 0$$
$$\frac{k_c q_{1n} q_{2n}}{4} + k_c q_{2n} q_{0n} + 3\Omega^2 = 0$$

where the subscript n denotes a normalized quantity. Assuming spherical spacecraft we can use Gauss' Law to relate the vehicle surface potential in volts to the equivalent encircled point charge q_i as $V_i=q_i/4pe_0r_i$ where r_i is the spacecraft radius. In a loosely analogous fashion we will define a normalized voltage V_{in} based on the normalized charge q_{in}

Eqn. 12
$$V_{in} \equiv k_c q_{in}$$

then the equilibrium equations of Eqn. 11 are

Eqn. 13
$$V_{1n} V_{2n} + 4V_{1n} V_{0n} + 12k_c\Omega^2 = 0$$
$$V_{1n} V_{2n} + 4V_{2n} V_{0n} + 12k_c\Omega^2 = 0$$

These are readily solved analytically. Given a suitable combiner spacecraft normalized voltage, V_{0n}, the two collector normalized voltages must be equal and are

Eqn. 14
$$V_{1n} = V_{2n} = -2V_{0n} \pm 2\sqrt{V_{0n}^2 - 3k_c\Omega^2}$$

where the combiner normalized voltage must satisfy the constraint

Eqn. 15
$$V_{0n}^2 - 3k_c\Omega^2 \geq 0$$

Knowing the actual collector mass, m, radius, r, separation, L, and the orbital angular rate W, the equilibrium collector physical voltage can be obtained from Eqn. 14 and the normalization relationship

Eqn. 16
$$V_{in} = \frac{V_i r_i}{\sqrt{mL^3}}$$

where the quantity $V_i r_i$ (which is equal to $q_i/4pe_0$ by Gauss' Law) is called the *reduced charge* of spacecraft i. The normalized collector voltages, obtained from Eqn. 14, are shown in Figure 9 as a function of the combiner voltage, V_{0n}. The angular rate Ω is for a geosynchronous orbit, $\Omega = 7.2915\times10^{-5}$ rad/s. Similar analytic methods were used to compute the y- and z-axis aligned formations. These solutions are also shown in Figure 9.

The three-spacecraft solution set yield some interesting insight. The most trivial case is the y-axis geometry. For this alignment within the Hill's system, a solution set is possible where all of the vehicles are uncharged. Indeed, if any vehicle has a non-zero charge, the net effect of the solution is to exactly cancel the effect of this charge such that the net force is always zero. The z-axis formation permits solutions where the central combiner has no charge, however there is no solution where all vehicles are neutral and Coulomb forces are required to maintain the static equilibrium. Lastly, the x-axis formation does not permit any solutions with uncharged spacecraft. There is a clear minimum magnitude for V_{0n} (about 20 in the normalized units) below which no solution is possible.

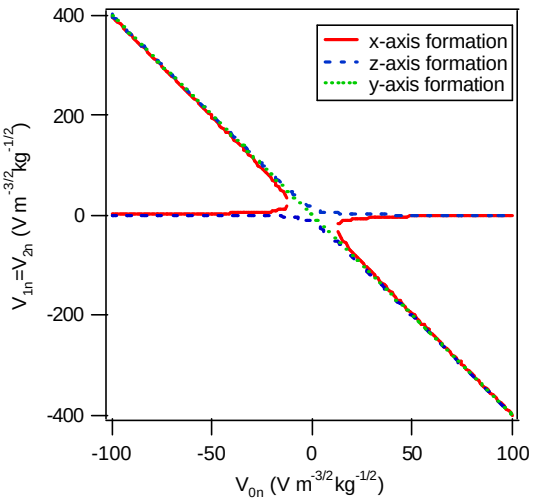

Figure 9. Analytic solution set for equilibrium three-spacecraft linear formations.

The analytic method was extended to the five-spacecraft two-dimensional formation and the seven-spacecraft three-dimensional formation.

When the constraints of the two- and three-dimensional formations were applied to the equilibrium requirements of Eqn. 6, the result was, respectively, eight and eighteen unique necessary conditions for equilibrium.

The two-dimensional five-spacecraft formation yielded two families of solutions. The first family was somewhat trivial and produced solutions where two of the vehicles had zero charge, such that the remaining vehicles assumed the same three-spacecraft linear solutions described above. The second family of solutions was found by forcing the symmetry condition that $q_1=q_3$ and $q_2=q_4$; this reduced the set of eight unique conditions to two.

Eqn. 17

$$4V_{0n}V_{3n} + V_{3n}^2 + 2\sqrt{2}V_{3n}V_{4n} - k_c\Omega^2 = 0$$
$$4V_{0n}V_{4n} + V_{4n}^2 + 2\sqrt{2}V_{3n}V_{4n} = 0$$

Eqn. 17 can be solved conditionally such that q_1 (and, hence q_3) have the form $q_1=q_1(q_4)$ and $q_0=q_0(q_1,q_4)$. The resulting solution set is shown in Figure 10. The solid and dashed lines represent consistent solutions within the set. For example, if $V_{2n}=V_{4n}$=-50, then *either* $V_{1n}=V_{3n}$=-10 with V_{0n}=20, *or* $V_{1n}=V_{3n}$=-50 with V_{0n}=50

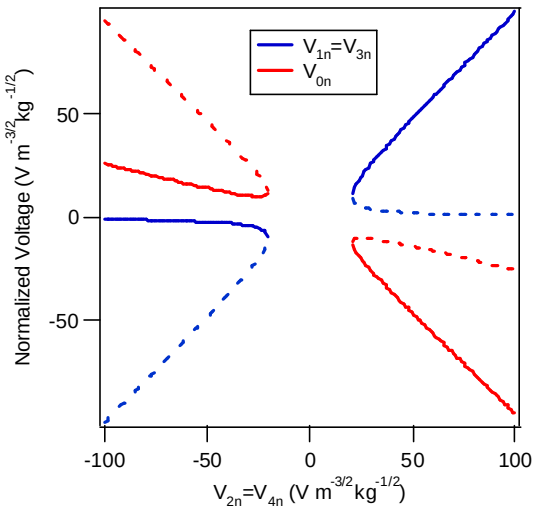

Figure 10. Solution set for equilibrium five-spacecraft two-dimensional formation.

The seven-spacecraft equilibrium solution was found by requiring the symmetry condition that $q_1=q_3$, $q_2=q_4$, and $q_5=q_6$, reducing the set of eighteen conditions to three unique equations:

Eqn. 18

$$\frac{k_c}{L^2}q_0q_1 + \frac{\sqrt{2}}{2L^2}k_cq_1q_2 + \frac{k_cq_1^2}{4L^2} + \frac{\sqrt{2}}{2L^2}k_cq_1q_5 - mL\Omega^2 = 0$$
$$\frac{1}{L^2}k_cq_0q_2 + \frac{\sqrt{2}}{2L^2}k_cq_1q_2 + \frac{1}{4L^2}k_cq_2^2 + \frac{\sqrt{2}}{2L^2}k_cq_2q_5 = 0$$
$$\frac{k_cq_0q_5}{L^2} + \frac{\sqrt{2}}{2L^2}k_cq_2q_5 + \frac{\sqrt{2}}{2L^2}k_cq_1q_5 + \frac{k_cq_5^2}{4L^2} + 3mL\Omega^2 = 0$$

Assuming a value of q_2 (or similarly q_4), Eqn. 18 can be solved analytically such that the collectors' charges are functions of q_2

Eqn. 19

$$q_1 = q_3 = q_1(q_2)$$
$$q_5 = q_6 = q_5(q_2)$$

The combiner charge, q_0, can then be expressed as $q_0 = q_0(q_1, q_2, q_5)$. A plot of the equilibrium solution set is shown in Figure 11. In the figure, solid and dashed lines represent consistent solutions within the set. For example, if V_{2n} is –50, then the solution is *either* $V_{1n}=V_{3n}$=-50, $V_{5n}=V_{6n}$=-60, with V_{0n}=75 *or* $V_{1n}=V_{3n}$=-10, $V_{5n}=V_{6n}$=8, with V_{0n}=10.

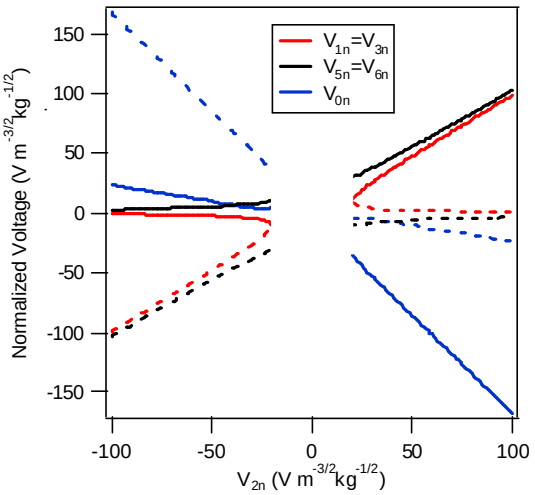

Figure 11. Equilibrium solution set for seven-spacecraft three-dimensional formation.

3.4. Physical Estimates

The normalized and reduced variables utilized in the analytic solution method can be used to estimate physically meaningful parameters. It is apparent from a study of Figure 9, Figure 10, and Figure 11 that an infinite number of possible vehicle charge states (voltages) exist for any of the

formations. One method of selecting an "optimal" set of parameters was based on minimizing the overall charging required by the formation. Using the sum of the squares of the vehicle charges as a cost function, the optimum solution for each formation was calculated analytically. The optimal solutions can be used to provide estimates of physical parameters. For discussion sake, it is assumed here that the vehicles each have identical mass of 150 kg, and that the inter-spacecraft separation for all of the formations was L=10 m. From the optimum solutions the value of reduced charge, $V_i r_i$, can be calculated. The reduced charge can be thought of as the surface potential required for a spherical vehicle with 1-m-radius, with scaling to different radii vehicles a straightforward calculation. The magnitude of optimal vehicle reduced charge for each formation is presented in Table 4.

	V_0r_0	V_1r_1	V_2r_2	V_3r_3	V_4r_4	V_5r_5	V_6r_6
3-x	13.8	13.8	13.8				
3-z	2.39	2.39	2.39				
5	4.78	3.96	7.92	3.96	7.92		
7	12.7	3.96	7.92	3.96	7.92	11.2	11.2

Table 4. Minimum total charge equilibrium solutions for each of the formations. For the linear formations, only the x-axis aligned and z-axis aligned three-spacecraft solutions are shown. The units of the vehicle reduced charges (V_ir_i) are in kV-m. The numbers can be thought of as the surface potential of a 1-m-radius spherical spacecraft in kilovolts.

4. Propulsion Figures of Merit

The purpose of this section is to evaluate some fundamental performance metrics of a Coulomb control system on a spacecraft formation. Aspects such as control force, input power, required consumable mass, and environment interaction will be calculated for a simple two-spacecraft system.

4.1. Required Power

An isolated spacecraft will assume an equilibrium potential (voltage) such that the net environmental current due to plasma and photoelectron emission is zero. It is possible to change the vehicle potential by emitting charge from the spacecraft. For example, if it is desired to drive the spacecraft potential lower than equilibrium (more negative), the emission of positive ions from the vehicle will cause a net surplus of on-board electrons and a lowering of the potential. In order to emit such a current, the charges must be ejected from the vehicle with sufficient kinetic energy to escape the spacecraft potential well. Thus, if the vehicle as at a (negative) potential $-V_{SC}$, then ions must be emitted from a source operating at a power supply voltage, V_{PS}, greater than $|-V_{SC}|$.

Basic concepts can be used to calculate the power required to maintain the spacecraft at some steady state potential. To maintain the spacecraft at a voltage of $|V_{SC}|$, current must be emitted in the amount of $|I_e| = 4\pi r^2|J_p|$, where J_p is the current density to the vehicle from the plasma, using a power supply having voltage of at least $|V_{PS}| = |V_{SC}|$. Quantitatively,

Eqn. 20 $$P = \left|V_{SC} I_e\right|.$$

For a two-spacecraft formation with each vehicle using Power P, the total system power is just the sum of the individual power to each vehicle. Assuming spherical spacecraft and using Gauss' Law to relate the surface potential to the encircled point charge, it is possible to relate the Coulomb force (thrust) on a vehicle to the emission current and the required power

Eqn. 21 $$F_C = 4\pi\varepsilon_0 e^{-d/\lambda_d} \frac{r_A r_B P^2}{d^2 I_{eA} I_{eB}}$$

where $r_{A(B)}$ and $I_{eA(B)}$ are the radius and emission current of spacecraft A(B), and d is the vehicle separation.

Eqn. 21 yields the power required to produce a steady-state thrust for a given emission current. Since the space environment will be constantly changing (and, hence the emission current to maintain steady state), it is important to calculate the required power to affect a change in potential from some initial value to a desired steady state value. In the pedagogical analysis here, the capacitance of the spherical spacecraft can be used to estimate the power required for a change in voltage (thrust). Using an equivalent circuit model where $dV_{SC}/dt = I/C$, the rate of change of spacecraft potential can be related to the current absorbed from the plasma and the emitted control current

Eqn. 22 $$\frac{dV_{SC}}{dt} = \frac{4\pi r^2 J_p + I_e}{4\pi\varepsilon_0 r}$$

where J_p is the absorbed plasma current density. The value of J_p can easily be evaluated using traditional plasma probe theory for a sphere and will take the form $J_p = J_p(V_{SC}, T_e, T_i)$. If V_{final} is the desired steady state spacecraft voltage, then the emission current power supply must have power $P = I_e V_{final}$. Substituting $I_e = P/V_{final}$ into Eqn. 22 and

using an analytic form for the plasma current, an explicit equation is obtained of the form

Eqn. 23 $$\frac{dV_{SC}}{dt} = f\left(P, V_{SC}, T_e, T_i, r\right)$$

which can be numerically integrated to produce a function

Eqn. 24 $$V_{SC} = V_{SC}\left(T_e, T_i, r, P, t\right).$$

As a numerical example, Figure 12 shows a plot of the function obtained for Eqn. 24 assuming a 1-m-diameter spacecraft charging from V_{SC}=0 to V_{final}=6 kV in the average GEO plasma environment. From this plot it is evident that only 200 mW of power is required to change the spacecraft potential by 6 kV within 8 msec.

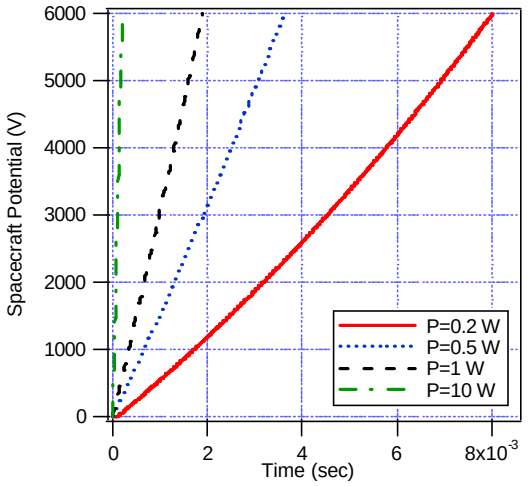

Figure 12. Numerical integration of the transient response of a 1-m-diameter model spacecraft in an average GEO plasma as a function of the power in the emitted control beam.

4.2. Mass Flow Rate and I_{sp}

Mass flow rate is defined by the rate of gaseous ions expelled out per unit time to maintain potential of the vehicle. As electrons have negligible mass we can say that mass flow rate of electrons is negligible and thus driving the potential positive requires zero mass flow. If I_e is the emission current constituting ions, m_{ion} is the mass of ion, and q_{ion} is the charge, then mass flow rate is given by

Eqn. 25 $$\dot{m} = \frac{I_e m_{ion}}{q_{ion}}.$$

Since the only purpose of the ion emission is to carry charge (and not momentum) from the vehicle, it makes sense to use the least massive ions that are practical. For a two spacecraft combination, propellant mass flow rate will be the sum of mass flow rates for individual spacecraft and can be related to their individual emission currents

Eqn. 26 $$\dot{m}_{Total} = \frac{m_{ion}}{q_{ion}}\left(I_{ea} + I_{eB}\right).$$

A common performance parameter used for propulsion systems is specific impulse I_{sp}. This parameter compares the thrust derived from a system to the required propellant mass flow rate.[24] Although I_{sp} is traditionally used as a parameter to evaluate momentum transfer (rocket) systems, we can use the formal definition to compare the Coulomb system. For a Coulomb control system the specific impulse I_{sp} is given by

Eqn. 27 $$I_{sp} = \frac{F}{\dot{m}_{Total} g_0}$$

Since Coulomb force calculations are meaningless for a single vehicle, we will treat the system as two separate vehicles, each subject to a force of F_c given by Eqn. 21, so that the sum of the forces experienced by all spacecraft in the formation is $F=2F_c$.

Eqn. 28

$$I_{sp} = \frac{8\pi\varepsilon_0 e^{-d/\lambda_d} q_{ion}}{g_0 m_{ion}} \frac{r_A r_B P^2}{d^2 I_{eA} I_{eB}\left(I_{eA} + I_{eB}\right)}$$

Where g_0 is the gravitational constant. If $r_A = r_B = r_{sc}$, and $I_e = I_{eA} = I_{eB}$, then Eqn. 28 becomes,

Eqn. 29 $$I_{sp} = \frac{4\pi\varepsilon_0 e^{-d/\lambda_d} q_{ion} r_{SC}^2 P^2}{g_0 m_{ion} d^2 I_e^3}.$$

Note that, unlike a rocket system, the definition of I_{sp} of a coulomb system is meaningless for a single vehicle. For a formation of two spacecraft, Eqn. 29 indicates that the specific impulse of the formation is a function of the radii of the spacecraft, power supplied to the ion (electron) gun, the separation between the two spacecraft, the emission currents of both vehicles, and the mass of the charge carriers, m_{ion}.

Consider a two-spacecraft formation with identical 1-m-diameter vehicles in the average GEO plasma environment charged to the same

negative potential. In order to reach and maintain this negative potential, the vehicles must emit an ion current. Consequently, the spacecraft will attract ion saturation current from the plasma, so I_e must be equal to the plasma ion saturation current for steady state. It is apparent that light ions will provide the most efficient I_{sp}, so assume that the emitted species is H^+. Calculated values of specific impulse for each vehicle in the formation is shown in Figure 13 for various system input power levels. For 1 mW systems with vehicle separation on the order of 20 m, I_{sp} values of 10^4 seconds are obtained, with values increasing to 10^{10} sec for just 1 W of power. It should be noted that for a positive vehicle potential the emitted species would be electrons and, thus, the calculated values of I_{sp} would be a factor of 2,000 greater.

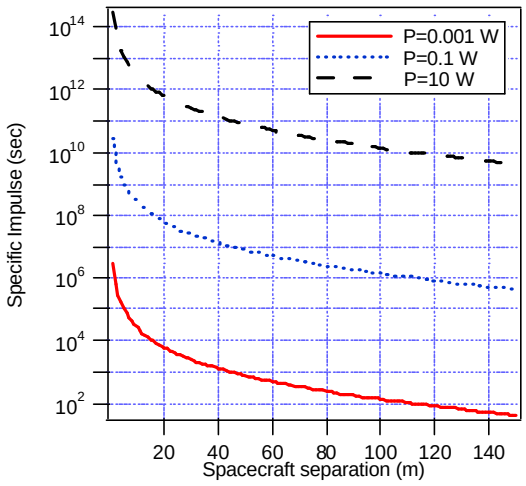

Figure 13. Specific impulse for a two-spacecraft Coulomb formation as a function of spacecraft separation, d, and input power, P.

4.3. Emission Current Jet Force

Generating net charge on a spacecraft for Coulomb force requires the emission of current. In principle, the charge is carried away from the vehicle by particles with non-zero mass. Such mass ejection results in a momentum jet force on the vehicle as in a traditional electric propulsion thruster. In the case of electron emission, the mass of the charge carriers is insignificant and the resulting jet force is negligible. Ion emission, however, may produce a significant reaction force. It is instructive to consider how the Coulomb force between spacecraft compares with the momentum reaction on the vehicle induced by the beam of ion current.

The reactive thrust force of an ejected mass flow is computed as

Eqn. 30
$$F_J = \dot{m} u_e ,$$

where $\dot{m}$ is the ejected mass flow rate and u_e is the exhaust velocity at which the mass is emitted. Assuming steady state Coulomb force generation, the ions will be electrostatically accelerated through a spacecraft potential of V_{SC}, such that

Eqn. 31
$$u_e = \sqrt{\frac{2 q_{ion} V_{SC}}{m_{ion}}} .$$

With this simplification and recognizing that the mass flow is related to the emission current, the momentum jet force of the emitted ion current is

Eqn. 32
$$F_J = I_e \sqrt{\frac{2 m_{ion} V_{SC}}{q_{ion}}} .$$

The jet force can also be written in terms of the input power to the emission system as

Eqn. 33
$$F_J = \sqrt{\frac{2 m_{ion} P I_e}{q_{ion}}} .$$

We can compare the magnitude of the jet reaction force with the induced Coulomb force between two vehicles. Assume identical spacecraft charged to the same value of V_{SC}. From Eqn. 21 and Eqn. 33 we can write the ratio of F_C/F_J (taking F_c as the total Coulomb force on both vehicles) in terms of the input power as

Eqn. 34
$$\frac{F_C}{F_J} = 4\sqrt{2}\pi\varepsilon_0 \sqrt{\frac{q_{ioin}}{m_{ion}}} \frac{r_A r_B P^{3/2} e^{-d/l_d}}{I_{eA} I_{eB} (I_{eA} + I_{eB}) d^2} .$$

If $r_A = r_B = r_{sc}$, and $I_e = I_{eA} = I_{eB}$ then Eqn. 34 becomes,

Eqn. 35
$$\frac{F_C}{F_J} = 2\sqrt{2}\pi\varepsilon_0 \sqrt{\frac{q_{ion}}{m_{ion}}} \frac{r_{SC}^2 P^{3/2} e^{-d/l_d}}{I_e^3 d^2} .$$

For a formation of two spacecraft, we find that the F_C/F_J ratio is a function of the radii of the spacecraft, power supplied to the ion (electron) gun, the separation between the two spacecraft and the emission currents of both of them. Similar to the calculations for specific impulse, if we consider

formation of two identical spacecraft in GEO having same diameter of 1 m, charged to same high negative voltage V_{SC} and provided with same power P for each of them, they will each draw ion saturation current from the ambient plasma. So the (ion) emission current I_e will be also the same. Figure 14 shows the ratio of Coulomb to jet force assuming hydrogen ion emission in average GEO plasma.

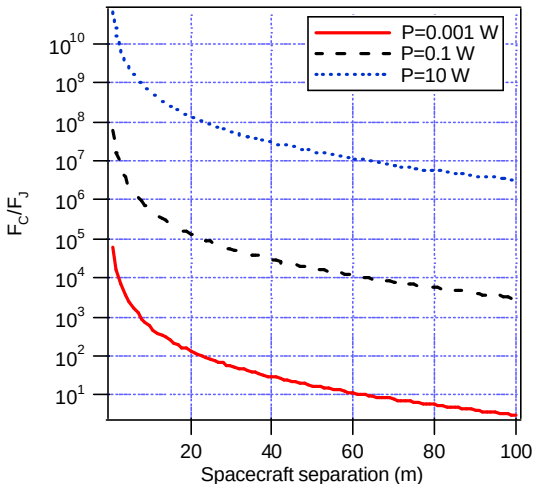

Figure 14. Comparison between induced Coulomb force and the momentum reaction of the emitted ion beam used to maintain the spacecraft charge for three power levels.

It can be seen from Figure 14 that for separations up to 100 m and system power greater than 1 mW the Coulomb force is considerably higher than the jet force. This implies two conclusions: 1) the Coulomb force is a wiser use of power than a mass-emitting EP thruster, and 2) the directional jet force will not be a significant perturbation to the Coulomb control system.

5. Conclusions

A new mode of potential spacecraft interaction was identified for closely spaced formations of vehicles in high Earth orbit. Using typical GEO conditions found in the literature, modeling and calculations were performed to show that Coulomb forces between vehicles may be as large as 1 mN for spacecraft 10 m apart, with electric dipole disturbance torques as high as 100 μN-m at the closest separations. For larger spacing most models showed the potential for forces of tens of μN and μN-m torques persisting out to 50 m separation.

The Coulomb disturbance forces are commensurate with those expected from micropropulsion systems that will likely be used for formation maintenance. In an exploratory study, the possibility to purposefully exploit the Coulomb interactions as formation-keeping forces was investigated. The dynamic equations were formed within Hill's relative coordinate system for a collection of interacting vehicles. Analytic methods were developed to prove the existence of static equilibrium solutions using only Coulomb forces for propulsion within the swarm. Unique solution sets were found for one-dimensional three-spacecraft formations, a two-dimensional five-spacecraft formation, and a three-dimensional seven-spacecraft formation. Assuming 150-kg vehicles with physical dimensions of 1 meter, it was shown that kilovolt spacecraft potentials are sufficient to maintain most formations in a rigid geometry.

The Coulomb control system was evaluated in classical propulsion terms. It was shown that the specific impulse can be as high as 10^{13} seconds. Due to the novel scaling of thrust, power, and specific impulse in this non-momentum thrust system, power levels as low as tens of milliwatts were shown sufficient to maintain the forces and to change their magnitude within a timescale of milliseconds.

6. Acknowledgements

Work reported here was supported by the NASA Institute for Advanced Concepts under a Phase I contract. This support is gratefully acknowledged.

7. References

[1]Pollard, J.E., Chao, C.C., and Janson, S.W., "Populating and maintaining cluster constellations in low-earth orbit," AIAA-99-2878, AIAA Meeting Papers on Disk Vol. 4, No. 3, Proc. Of 35th AIAA/ASME/SAE/ASEE Joint Propulsion Conference, June 20-24, 1999, Los Angeles, CA.

[2]Walker, J.G., "The geometry of cluster orbits," J. Brit. Interplan. Soc., Vol. 35, 1982, p. 345.

[3]Murdoch, J. and Pocha, J.J., "The orbit dynamics of satellite clusters," Paper IAF-82-54,

33rd International Astronautical Congress, Sept. 27-Oct. 2, 1982, Paris, France.

[4]Chao, C.C., Pollard, J.E., and Janson, S.W., "Dynamics and control of cluster orbits for distributed space missions," Paper AAS-99-126, Space Flight Mechanics Meeting, Feb. 7-10 1999, Breckenridge, CO.

[5]Kong, E.M.C., Miller, D.W., and Sedwick, R.J., "Exploiting orbital dynamics for aperture synthesis using distributed satellite systems: Applications to a visible Earth imager system," Paper AAS-99-122, Space Flight Mechanics Meeting, Feb. 7-10 1999, Breckenridge, CO.

[6]Sedwick, R., Miller, D., and Kong, E., "Mitigation of differential perturbations in clusters of formation flying satellites," Paper AAS-99-124, Space Flight Mechanics Meeting, Feb. 7-10 1999, Breckenridge, CO.

[7]Miller, D.W. and Spores, R.A., "Proceedings of the Formation Flying and Micropropulsion Workshop," unpublished, Oct. 20-21 1998, available from Dr. Ronald Spores, Air Force Research Laboratory, Edwards AFB, CA.

[8]Micci, M.M. and Ketsdever, A.D., Micropropulsion for Small Spacecraft, Progress in Astronautics and Aeronautics, Vol. 187, AIAA Press, Reston, VA, 2000.

[9]Corazzini, T., Robertson, A., Adams, J.C., Hassibi, A., and How, J.P., "GPS sensing for spacecraft formation flying," Proceedings of the 10th International Technical Meeting, ION/GPS, Sept. 16-19 1997, Kansas City, MO.

[10]Vassar, R.H. and Sherwood, R.B., "Formationkeeping for a pair of satellites in a circular orbit," Journal of Guidance, Control, and Dynamics, Vol. 8, No. 2, 1985.

[11]Leonard, C.L., "Fuel penalty of using ballistic coefficient control for satellite formationkeeping," AAS 13th Annual Guidance and Control Conference, Keystone, CO, Feb. 1990.

[12]Jilla, Cyrus D., Separated Spacecraft Interferometry – System Architecture Design and Optimization, Master's Thesis, Dept. of Aeronautics and Astronautics, Massachusetts Institute of Technology, Feb. 1999.

[13]Kong, Edmund M., Optimal Trajectories and Orbit Design for Separated Spacecraft Interferometry, Master's Thesis, Dept. of Aeronautics and Astronautics, Massachusetts Institute of Technology, Nov. 1998.

[14]Yashko, Gregory, Ion Micro-Propulsion and Cost Modelling for Satellite Clusters, Master's Thesis, Dept. of Aeronautics and Astronautics, Massachusetts Institute of Technology, June 1998.

[15]Hacker, Troy L., Performance of a Space-based GMTI Radar System using Separated Spacecraft Interferometry, Master's Thesis, Dept. of Aeronautics and Astronautics, Massachusetts Institute of Technology, May 2000.

[16]Hastings, D., and Garret, H., Spacecraft-environment Interactions, Cambridge University Press, 1996, pp. 44-71.

[17]Garrett H. B., and DeFrost, S. E. "An analytical simulation of the geosynchronous plasma environment", Planetary Space Science, 27:1101-09, 1979.

[18]Garrett H. B., Schwank, D. C., and DeFrost, S. E " A statistical analysis of the low energy geo-synchronous plasma environment –I. electrons, Planetary Space Science, 29:1021-44, 1981a.

[19]Garrett H. B., Schwank, D. C., and DeFrost, S. E " A statistical analysis of the low energy geo-synchronous plasma environment –I. protons, Planetary Space Science, 29:1045-60, 1981b.

[20]Mullen, E. G., Gussenhoven, M. S., and Hardy, D. A. SCATHA survey of high-voltage spacecraft charging in sunlight, "Journal of Geophysical Research", 91:1474-90, 1986.

[21]Maxwell Technologies System Division, " Interactive Spacecraft Charging Handbook", Space Environment Effect Program, NASA Marshall Space Flight Center.

[22]Chong, Jer-Hong, Dynamic Behavior of Spacecraft Formation Flying using Coulomb Forces, Department of Mechanical Engineering-Engineering Mechanics, Michigan Technological University, May 2002.

[23]Kong, E.M., "Optimal Trajectories and Orbit Design for Separated Spacecraft Interferometry,"

Master's Thesis, MIT Dept. of Aeronautics and Astronautics, November, 1998.

[24]Ronald W. Humble, Gary N. Henry, Wiley J. Larson, "Space Propulsion Analysis And Design, revised", Space Technology Series, 1995, pp10.